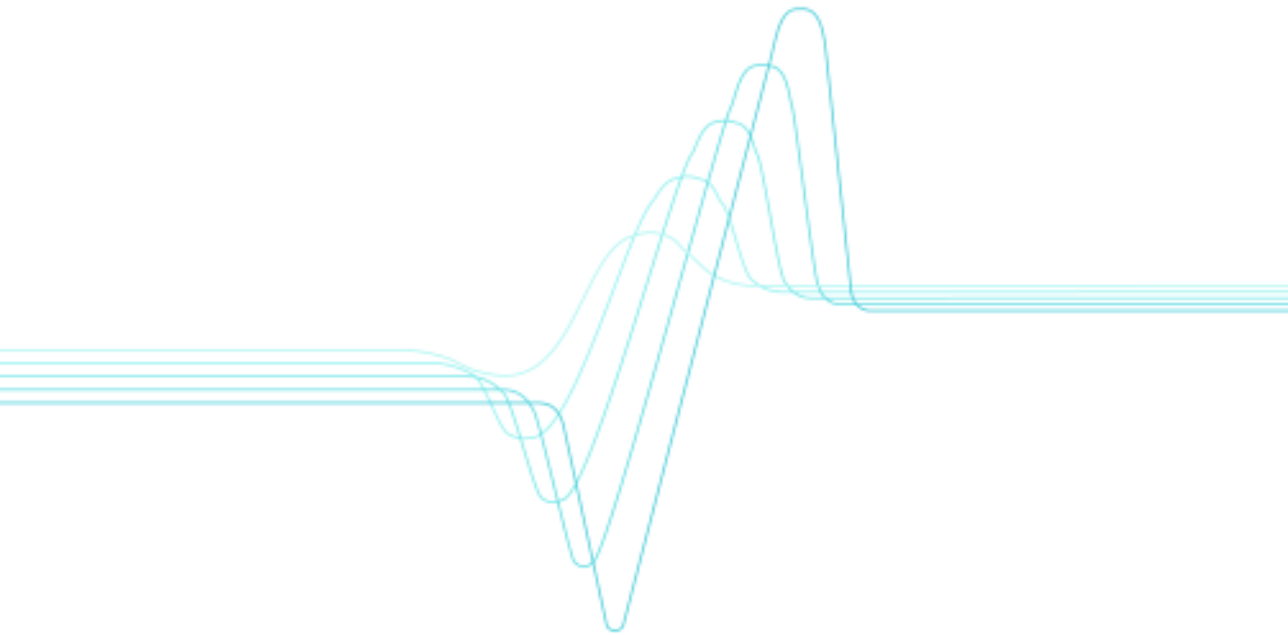


Ulrika Backman

# Studies on nanoparticle synthesis via gas-to-particle conversion





# **Studies on nanoparticle synthesis via gas-to-particle conversion**

Ulrika Backman

VTT Processes

Department of Physical Sciences  
Faculty of Science  
University of Helsinki  
Helsinki, Finland

Academic dissertation

*To be presented, with the permission  
of the Faculty of Science of the University of Helsinki, for public  
criticism in auditorium E207, Gustaf Hällströmin katu 2, Helsinki  
on May 20<sup>th</sup>, 2005, at 12 noon.*



ISBN 951-38-6441-3 (soft back ed.)

ISSN 1235-0621 (soft back ed.)

ISBN 951-38-6442-1 (URL: <http://www.vtt.fi/inf/pdf/>)

ISSN 1455-0849 (URL: <http://www.vtt.fi/inf/pdf/>)

Copyright © VTT Technical Research Centre of Finland 2005

JULKAISIJA – UTGIVARE – PUBLISHER

VTT, Vuorimiehentie 5, PL 2000, 02044 VTT

puh. vaihde 020 722 111, faksi 020 722 4374

VTT, Bergsmansvägen 5, PB 2000, 02044 VTT

tel. växel 020 722 111, fax 020 722 4374

VTT Technical Research Centre of Finland, Vuorimiehentie 5, P.O.Box 2000, FI-02044 VTT, Finland

phone internat. +358 20 722 111, fax + 358 20 722 4374

VTT Prosessit, Biologinkuja 7, PL 1602, 02044 VTT

puh. vaihde 020 722 111, faksi 020 722 7021

VTT Processer, Biologgränden 7, PB 1602, 02044 VTT

tel. växel 020 722 111, fax 020 722 7021

VTT Processes, Biologinkuja 7, P.O.Box 1602, FI-02044 VTT, Finland

phone internat. +358 20 722 111, fax +358 20 722 7021

Backman, Ulrika. Studies on nanoparticle synthesis via gas-to-particle conversion. Espoo 2005. VTT Publications 562. 45 p. + app. 62 p.

**Keywords** nanoparticle synthesis, gas-to-particle conversion, silver nanoparticles, supported metal catalyst nanoparticles, ruthenium dioxide nanorods, aerosol dynamics, characteristics, modelling, deposition, narrow size distribution

## Abstract

In this thesis the synthesis of nanoparticles via gas-to-particle conversion was studied both experimentally and theoretically. In the experimental part, nonagglomerated silver nanoparticles were produced via evaporation-condensation. It was shown that it is possible to control the particle size and degree of agglomeration using dilution. A new one-step process for synthesis of supported metal catalyst nanoparticles was developed. The carrier was produced via thermal decomposition of a metalorganic precursor and the metal was added via evaporation-condensation. The metal was well dispersed in 1–2 nm sized particles on the surface of the agglomerated carrier particles.

A simple system was also developed for depositing single nonagglomerated nanoparticles with a narrow particle size distribution. The system relied on the competition between diffusion and negative thermophoresis. Ruthenium dioxide nanorods were synthesised via decomposition of ruthenium tri- and tetroxide vapours. However, since no optimisation of the system was done, the size distribution was broad.

In the modelling part of this thesis the formation of silver nanoparticles via evaporation-condensation was studied. The modelling was done using two different approaches. In the first approach the classical nucleation theory and a sectional model were used, whereas in the second approach a discrete model was used and the nucleation was described as a dimerisation process. The results showed that for the classical nucleation theory to predict the final particle properties in the various cases, very different correction factors, 1–15 000, were needed. The kinetic nucleation approach gave better agreement between the model and experimental results.

# Preface

The work in this thesis has been carried out in the Fine Particle Group at VTT Processes. I am grateful for the guidance and support of my supervisors Professor Jorma K. Jokiniemi and Professor Kari E. J. Lehtinen. I also wish to thank Professor Markku Kulmala for guidance and the pre-examiners of this thesis, Professor Kaarle Hämeri and Docent Jyrki Mäkelä, who both gave valuable comments on this work.

I am grateful to my co-authors. Especially, to Mr. Ari Auvinen for the guidance on how to build experimental setups and for discussions and help with interpreting results. Dr. Unto Tapper is acknowledged for microscopy analyses and Mrs. Riitta Zilliacus and Mrs. Maija Lipponen for carrying out chemical analyses. The help and expertise of Mr. Raoul Järvinen in building experimental setups is highly appreciated. I would also like to thank all my colleagues at VTT for creating a pleasant working atmosphere.

This research was funded by VTT Processes, NKS (Nordic Nuclear Safety Research), IVO-Foundation and STUK (Radiation and Nuclear Safety Authority Finland). The financial support is gratefully acknowledged.

Finally, Petri deserves hugs for support, patience and valuable comments on the work. I would also like to thank 'Arne' for setting a firm deadline and kicking me to finish this thesis.

## List of papers

- I Backman, U., Jokiniemi, J. K., Auvinen, A. and Lehtinen, K. E. J. 2002. The effect of boundary conditions on gas-phase synthesised silver nanoparticles. *Journal of Nanoparticle Research*, Vol. 4(4), p. 325–335.
- II Lehtinen, K. E. J., Backman, U., Jokiniemi J. K. and Kulmala, M. 2004. Three-body collisions as a particle formation mechanism in silver nanoparticle synthesis. *Journal of Colloid and Interface Science*, Vol. 274(2), pp. 526–530.
- III Backman, U., Tapper, U. and Jokiniemi, J. K. 2004. An aerosol method to synthesize supported metal catalyst nanoparticles. *Synthetic Metals*, Vol. 142(1–3), pp. 169–176.
- IV Backman, U., Auvinen, A. and Jokiniemi, J. K. 2005. Deposition of nanostructured titania films by particle assisted MOCVD. *Surface and Coatings Technology*, Vol. 192(1), pp. 81–87.
- V Backman, U., Lipponen, M., Auvinen, A., Tapper, U., Zilliacus, R. and Jokiniemi, J. K. On the transport and speciation of ruthenium in high temperature oxidising conditions. Accepted for publication in *Radiochimica Acta*.

## Author's contribution

The research reported in this thesis was carried out in the Fine Particle Group at VTT Processes during the years 2000–2005 under the supervision of Prof. Jorma K. Jokiniemi and Prof. Kari E. J. Lehtinen.

In paper I nonagglomerated silver nanoparticles were synthesised via an evaporation-condensation method. The aerosol dynamics was modelled using the ABC-code. The author performed the experimental work and wrote most of the paper. The modelling was done by Prof. Jorma K. Jokiniemi, who also wrote the corresponding sections of the paper. The formation of silver nanoparticles was also modelled in paper II, using a kinetic model. This work was carried out by Prof. Kari E. J. Lehtinen, who also wrote most of the paper, assisted by the author.

In paper III titania-supported silver nanoparticles were synthesised. The author carried out the experimental work and wrote the paper. The microscopy analyses were carried out by Dr. Unto Tapper. In paper IV a system for deposition of nanoparticles with a narrow size distribution was developed. The author carried out the experiments, microscopy analyses and wrote the paper.

In paper V the behaviour of ruthenium at high temperature oxidising conditions was studied. The author carried out the experiments and wrote the paper. Interpretation of the results was done jointly with Mr. Ari Auvinen. The chemical analyses were done by Mrs. Maija Lipponen.

# Contents

Abstract.....	3
Preface .....	4
List of papers .....	5
Author's contribution .....	6
List of acronyms and symbols .....	9
1. Introduction.....	11
2. Synthesis of nanoparticles via aerosol methods.....	13
2.1 Nanoparticles.....	13
2.2 Aerosol methods for nanoparticle production .....	14
2.3 Aerosol dynamics .....	15
3. Experimental methods .....	18
3.1 Particle production.....	18
3.2 Characterisation methods .....	19
4. Modelling.....	21
4.1 Sectional method .....	21
4.2 Discrete method.....	22
5. Experimental results .....	24
5.1 Metal nanoparticles .....	25
5.2 Supported metal nanoparticles.....	28
5.3 Deposition of particles with narrow size distribution.....	30
5.4 Synthesis of RuO <sub>2</sub> nanorods .....	32
6. Modelling results .....	34
6.1 Sectional method .....	34
6.2 Discrete method.....	36

7. Conclusions.....	38
References.....	41

Appendices  
Papers I–V

*Appendices of this publication are not included in the PDF version. Please order the printed version to get the complete publication (<http://www.vtt.fi/inf/pdf>)*

## List of acronyms and symbols

BET	Brunauer-Emmett-Teller (method for measuring surface area)
CFD	computational fluid dynamics
CNC	condensation nucleus counter
CO	critical orifice
CVD	chemical vapour deposition
DMA	differential mobility analyser
ESP	electrostatic precipitator
GDE	general dynamic equation
ICP/AES	inductively coupled plasma atomic emission spectrometry
MFC	mass flow controller
MOCVD	metalorganic chemical vapour deposition
SAED	selected area electron diffraction
SEM	scanning electron microscope
TEM	transmission electron microscope
TTIP	titanium tetraisopropoxide
XRD	X-ray diffraction

$J$	nucleation rate
$k_{dep}$	deposition flux
$L$	probability
$n$	number density function
$N_1$	number concentration of monomers
$t$	time
$u, v$	particle volume
$\dot{\vec{x}}$	velocity vector
$\beta_{11}$	collision frequency function

# 1. Introduction

Nanoparticles are usually defined as particles less than 100 nm in diameter. They have different and often superior properties compared with those of bulk material. For instance, their chemical reactivity is higher, making them excellent material for use in sensor and catalysis applications [Ichinose et al. 1992, Edelstein and Cammarata 1996]. Nanoparticles are already used in many applications, e.g. in TiO<sub>2</sub>-based coatings on self-cleaning glass (Pilkington, PPG Industries) and in cosmetics as sunscreens and anti-ageing agents (L'Oréal, Lancôme). Financial analysts have estimated that the size of the nanoparticle market will be \$900 million in 2005 and \$11 billion in 2010 [Pitkethly 2003].

One convenient method for preparing nanoparticles is via the aerosol or gas phase routes. An aerosol is defined as a suspension of solid and/or liquid particles in a gas. Currently, pigments (TiO<sub>2</sub>), fumed silica and reinforcing agents (carbon black) are produced via aerosol methods on an industrial scale [Kodas and Hampden-Smith 1999, Swihart 2003]. Some reviews and books on gas phase synthesis of materials were recently published [Gurav et al. 1993, Hahn 1997, Kruis et al. 1998, Kodas and Hampden-Smith 1999, Swihart 2003].

In this thesis the production of nanoparticles via the gas phase routes was studied both experimentally and theoretically. The gas-to-particle route was employed to produce metallic as well as oxide nanoparticles in a tubular flow furnace. To control the size and shape and hence the properties of these particles, understanding of the mechanisms involved in particle formation is crucial. Therefore the tube furnace was modelled, using a detailed microphysical model including all relevant aerosol dynamic processes affecting the particle size distribution.

The objectives of this thesis were to investigate how quenching affects nanoparticle properties, to develop aerosol synthesis methods for supported metal nanoparticles as well as ruthenium dioxide nanorods, to develop a simple setup for the deposition of particles with a narrow size distribution and to study the nucleation and growth of silver nanoparticles in detail via modelling.

The work in this thesis was published in 5 papers. In paper I spherical nonagglomerated silver nanoparticles were produced using an evaporation-condensation method. Particle formation was modelled using the classical nucleation theory and the particle size distribution was described with a sectional method. In paper II the formation of Ag nanoparticles was also modelled, in which a discrete model was used to represent the particle size distribution and nucleation was described as a dimerisation process. This model was applied for the first time to nucleation in materials synthesis.

Traditionally, supported catalysts are prepared using wet chemistry. In these processes several steps such as drying and calcination are needed. In paper III a new one-step process for the production of metal oxide-supported catalyst nanoparticles was developed. The system was tested by producing Ag/TiO<sub>2</sub> particles, which have several applications, e.g. as catalysts and photocatalysts. The anatase phase is the more active phase in both applications. It has been shown that adding silver increases the photocatalytic activity of titania. The optimum amount of silver is between 0.5% and 4% [see e.g. Kondo and Jardim 1991, Vamathevan et al. 2001, He et al. 2002, Dobosz and Sobczynski 2003].

Since particles with a narrow size distribution are needed in many applications, a simple setup for deposition of nearly monodispersed particles was constructed in paper IV. The system relied on competition between diffusion and negative thermophoresis. Finally, in paper V, RuO<sub>2</sub> nanorods were synthesised via decomposition of gaseous RuO<sub>3</sub> and RuO<sub>4</sub>. These volatile species were formed from RuO<sub>2</sub> powder at high temperature oxidising conditions. This technique is generally referred to as the chemical vapour transport technique. RuO<sub>2</sub> has many interesting areas of application, e.g. as resistors, catalysts and electrochemical capacitors.

This thesis is organised as follows. In chapter 2 nanoparticles and the aerosol methods used to produce them are discussed. The key aerosol dynamics processes are also briefly presented. The experimental methods and analysis techniques employed in the thesis are described in chapter 3, whereas in chapter 4 the modelling tools used are briefly presented. In chapter 5 the most important experimental results are discussed. The key mechanisms involved in particle formation and growth processes in each case are discussed in detail. The modelling results are briefly discussed in chapter 6 and finally the conclusions are drawn in chapter 7.

## **2. Synthesis of nanoparticles via aerosol methods**

In the first part of this chapter the advantages and production methods of nanoparticles will be briefly addressed. Then a short overview of aerosol methods for production of nanoparticles will be given. The method used in this thesis, the gas-to-particle route, will be described in further detail. The advantages and drawbacks of the various production methods will also be discussed. Finally, the most important aerosol dynamics processes will be presented.

### **2.1 Nanoparticles**

Nanoparticles are commonly defined as particles less than 100 nm in diameter [Ichinose et al. 1992, El-Shall and Edelstein 1996]. Due to this small size, nanoparticles have a large fraction of surface atoms, i.e. a high surface-to-volume ratio. This increases the surface energy compared with that of bulk material. The high surface-to-volume ratio together with size effects (quantum effects) give nanoparticles distinctively different properties (chemical, electronic, optical, magnetic and mechanical) from those of bulk material. For instance, nanoparticle-based semiconductor sensors exhibit higher sensitivities to air pollutants and have lower detection thresholds and lower operating temperatures [Baraton and Merhari 2004]. In various applications e.g. electronic, magnetic and optical [Kruis et al. 1998], in bioanalysis [Penn et al. 2003] and in environmental remediation [Kamat and Meisel 2003, Zhang 2003], nanoparticles are used.

Nanoparticles can essentially be prepared in 3 different ways: via mechanical attrition, wet phase or gas phase methods. The properties of the final product may differ depending on the fabrication route. In mechanical attrition the bulk material is reduced in size via milling. This is a simple technique with low-cost equipment, however, it produces particles with a broad size distribution, and contamination from the milling machinery is often a problem. [Ichinose et al. 1992, Edelstein and Cammarata 1996, Tjong and Chen 2004]

In the wet phase methods, well-defined quantities of different ionic solutions are mixed. The conditions (temperature and pressure) are well controlled to promote the formation of insoluble compounds that precipitate out of the solution. To produce a dry powder, the precipitate is then filtered and/or spray-dried. With these methods a large variety of compounds can be fabricated using rather inexpensive equipment, however, bound solvent molecules can be a problem and the yield can be quite low. [Ichinose et al. 1992, Edelstein and Cammarata 1996, Pitkethly 2003, Tjong and Chen 2004]

## **2.2 Aerosol methods for nanoparticle production**

The aerosol methods for production of material particles can be divided into the gas-to-particle and the liquid/solid-to-solid routes. In the liquid/solid-to-solid route the product particles are formed from droplets or solid reactant particles via intraparticle reactions. Using this method it is possible to produce single- and multicomponent materials with controlled levels of doping with many elements. The chemical composition of the particles is homogeneous. It is a continuous process that can be scaled up. However, this is a complicated technique since many different physical and chemical phenomena (e.g. evaporation of the solvent, chemical reactions) can occur simultaneously. [Gurav et al. 1993, Kudas and Hampden-Smith 1999]

The gas-to-particle route is a commonly utilised method when nanoparticles are to be produced via aerosol methods. In this route, particles form via nucleation from a supersaturated vapour. Supersaturation can be achieved via physical processes such as cooling of a hot vapour or via chemical reactions of gaseous precursors, which results in the formation of condensable species. Solid, spherical or nearly spherical particles with narrow particle size distributions can be produced. Very small particles on the order of nanometres can be produced and the final product is often of high purity. However, the production rates may be low in some setups and multicomponent materials may be difficult to produce. There may also be problems with hazardous reactants and by-products. [Gurav et al. 1993, Kudas and Hampden-Smith 1999] The degree of agglomeration of the synthesised nanoparticles can be controlled by varying the process conditions, e.g. the initial concentration of precursor, maximum temperature, residence time and cooling rate [Tsantilis and Pratsinis 2004].

Particle formation from gaseous species is often divided into 2 routes: physical and chemical, depending on how the supersaturation needed for particle nucleation is achieved. However, they are identical in terms of the aerosol dynamics that occurs once the condensable species have formed. In the physical route, the solid precursor and the final product are the same material. This makes the route simple, since no chemical reactions occur in the gas phase. However, temperatures high enough to vaporise the precursor are needed, this limits the materials that can be processed. [Gurav et al. 1993, Kodas and Hampden-Smith 1999] Since the yield in evaporation-condensation synthesis of nanoparticles tends to be low, studies have been undertaken on how to increase it [Singh et al. 2002].

In the chemical route, the production rates can be significant if a precursor with high volatility is available. Therefore, chemicals such as metal chlorides or metalorganic compounds are often used; titania is produced on an industrial scale from  $TiCl_4$  using this method. However, in using metal chlorides or metalorganic compounds there is a possible risk of contaminating the final product. Chemical vapour deposition can occur on the walls of the system, which may decrease the yield in particle production. [Gurav et al. 1993, Kodas and Hampden-Smith 1999] Composite particles can be produced, using the chemical route. Various intraparticle structures (from core-shell to mixed-type) may be produced, depending on the mixing order of the reactants [Lee et al. 2002]. The precursor may affect the properties of the final product under constant processing conditions [Yoon et al. 2003], due to the differences in chemistry of the species involved.

## 2.3 Aerosol dynamics

Once a sufficiently high supersaturation is achieved as a result of formation of condensable species, nucleation occurs. After nucleation, particle growth can proceed in two different ways: via condensation or coagulation [Hinds 1999]. Growth via condensation occurs at low particle concentrations where few if any collisions occur. This is often the case in laboratory systems, where monomers condense onto the already existing particles, resulting in spherical particles. Growth via surface reaction can also occur [Kodas and Hampden-Smith 1999]. At high particle concentrations, particles grow via coagulation as they collide and coalesce. If coalescence is rapid, complete fusion can occur before the next

collision, thus producing spherical particles, this growth mode is termed collision-limited growth. However, if coalescence is slow and collisions occur before complete coalescence has been achieved, agglomerates are formed, this growth mode is termed coalescence-limited growth [Lehtinen et al. 1996]. In real systems conditions are seldom strictly collision- or coalescence-limited, but intermediate and so produce partially sintered nonspherical particles [Wu et al. 1993].

It is important to understand the transport of particles in the gas phase, because it decreases the yield in particle production due to deposition. Transport phenomena are also important in collection of particles produced. In addition, these phenomena influence the properties of the particles.

All particles in the gas phase undergo Brownian diffusion, i.e. random motion due to collisions with gas molecules. Even though the motion is random at atomic scales, it results in net particle transport from regions of high to low concentration. Particles also collide with each other due to diffusion. The diffusion velocity is strongly dependent on particle size: the smaller the particles, the higher their diffusion velocity. Deposition via diffusion is important only for submicron particles and short distances. [Hinds 1999, Friedlander 2000]

Aerosol particles are also influenced by external fields. Particles in a thermal gradient experience a force, thermophoresis, in the direction of lower temperature, which makes the particles deposit in cold regions of the system. The thermophoretic velocity is nearly independent of particle size for submicron particles and is directly proportional to the thermal gradient. [Hinds 1999, Friedlander 2000]

The transport of charged particles in an electric field is referred to as electrophoresis. The electrophoretic velocity is inversely proportional to the particle size and directly proportional to the electric field and charge of the particle, which is also dependent on the particle size. Electrophoresis can be utilised when characterising, separating or depositing particles. [Hinds 1999, Friedlander 2000]

In gravitational fields particles settle, however, this becomes important only for particles larger than 1  $\mu\text{m}$  and is usually not an issue in gas-to-particle

conversion systems. Large particles can be collected using settling if sufficiently long residence times are allowed. However, in aerosol processing of materials the residence times are usually less than 1 min. [Hinds 1999, Friedlander 2000]

If no other forces influence the motion of the particles, they follow the gas streamlines. However, if the gas stream changes direction, as for instance in a pipe bend, larger particles cannot keep up with the change in flow. Due to inertia they may continue in the original direction and impact. Particles larger than 1  $\mu\text{m}$  are mostly affected by inertial impaction. Inertial impaction is taken advantage of when collecting particles, e.g. in cyclones, and when classifying particles in inertial impactors. [Hinds 1999, Friedlander 2000]

### 3. Experimental methods

In this chapter the experimental setups used to produce nanoparticles via gas-to-particle conversion are briefly presented. The main characterisation methods used are also introduced.

#### 3.1 Particle production

A tubular flow furnace (Entech, ETF20/18-II-L) was used in all the experiments carried out in this thesis. The furnace was 110 cm long and had two heating zones, each 40 cm long. These zones were separated by a 38-mm layer of insulation. Since the furnace tube was heated through radiative heat transfer, there were 131 mm of thermal insulation at both ends. The inner diameter of the ceramic ( $\text{Al}_2\text{O}_3$ , 99.7%) furnace tube was 22 mm. The maximum temperature of the furnace was 1800°C and the system was operated at atmospheric pressure in all experiments. Flow rates between 5 and 10 l/min were used, corresponding to residence times of 0.9–0.4 s. A schematic of the experimental setup used to produce supported metal nanoparticles (paper III) is presented in Figure 1, all other setups were modifications of this system. The details are presented in the experimental sections of each paper.

The precursor feed was realised in two different ways, depending on the physical state of the precursor. In experiments with a solid-state precursor (Ag or  $\text{RuO}_2$  powder; papers I–III, V), it was placed in a ceramic ( $\text{Al}_2\text{O}_3$ , 99.7%) crucible, which was placed above either the first or the second heating block of the furnace. When using liquid titanium tetrakisopropoxide (TTIP) precursor (papers III, IV) it was fed from a temperature-controlled vaporiser, placed upstream of the furnace, by bubbling the carrier gas through. The lines from the vaporiser to the furnace were heated with heating tapes to prevent the vaporised precursor from condensing before reaching the furnace.

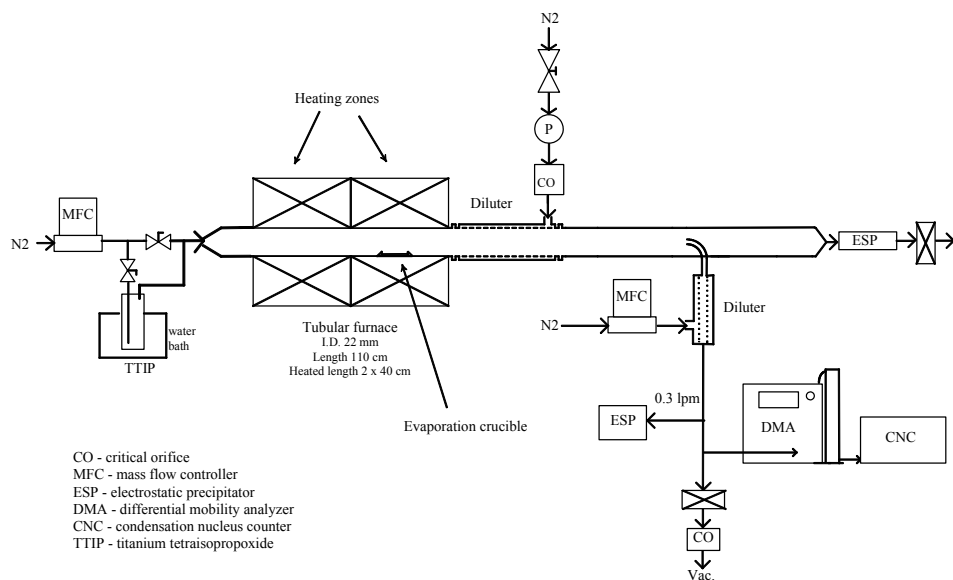


Figure 1. Schematic of experimental setup used to produce supported metal nanoparticles (paper III).

In some experiments (papers I–III) a porous tube diluter was placed directly downstream of the furnace to quench the exiting gas stream. The aerosol was diluted to promote the formation of small particles and to prevent agglomeration. In the porous tube diluter the aerosol flow is diluted with gas that flows through a porous tube into the inner tube. Using a porous tube diluter the losses resulting from diffusion and thermophoresis can be minimised [Auvinen et al. 2000]. Sampling of the particles produced was done downstream of the furnace using a j-shaped probe pointing upstream against the flow. The sample was diluted, using a porous tube diluter in all experiments.

### 3.2 Characterisation methods

The number size distribution of the nanoparticles produced was measured with a differential mobility analyser (DMA; TSI 3081 or 3085) [Knutson and Whitby 1975] and a condensation nucleus counter (CNC; TSI 3022 or 3025) [Agarwal and Sem 1978]. Before entering the DMA, the aerosol passes a preimpactor that removes the largest particles and a neutraliser (bipolar charger) in which the particles are charged to the Boltzmann equilibrium distribution. In the DMA the particles are separated

according to their electrical mobility in an electric field. At each voltage only particles within a narrow mobility range (and particle size) are able to exit the DMA. After exiting the DMA the aerosol enters the CNC, in which the particle concentration of each mobility fraction is measured. In the CNC the particles are grown by condensing butanol onto them, after which they are detected and counted optically. The system was used in the scanning mode [Wang and Flagan 1990] and controlled with the Aerosol Instrument Manager software version 4.0 (TSI).

Depending on the size of the particles produced in the experiments, either DMA model 3081 and CNC model 3022 or DMA model 3085 and CNC model 3025 were used to measure the number size distribution. The DMA model 3085 is optimised for particles less than 20 nm in size. It was designed to reduce the effects of diffusion by decreasing the residence time in the DMA [TSI 1999]. The first combination (DMA 3081, CNC 3022) can measure particles between 10 and 1000 nm in size, whereas the second combination (DMA 3085, CNC 3025) can measure particles between 3 and 150 nm. The concentration range is 2 to  $10^8$  particles/cm<sup>3</sup> and 20 to  $10^7$  particles/cm<sup>3</sup>, respectively [TSI 1990, TSI 1999]. In the experiments reported in papers I and II, DMA model 3085 and CNC model 3025 were used to measure the silver nanoparticles produced. In the other experiments the particles were larger and therefore DMA model 3081 and CNC model 3022 were used.

The particles were collected from the gas phase on carbon-coated copper grids using a point-to-plate electrostatic precipitator. These samples were used to analyse the morphology and crystallinity of the particles in a transmission electron microscope (TEM). The TEM used in this study was a Philips CM-200 FEG/STEM. A scanning electron microscope (SEM, Leo Gemini 982) was also used in papers IV and V to perform analysis.

Various other characterisation techniques were also used in this thesis. For instance, the crystallinity of the powder produced in paper III was analysed using X-ray diffraction (XRD), which relies on the interaction of X-rays with a crystalline material. This interaction can be described by Bragg's law, which relates the lattice spacing to the X-ray wavelength. The specific surface area of the samples was determined with the Brunauer-Emmet-Teller (BET) method, in which a gas (in this case nitrogen) is adsorbed onto the surface. The amount of gas adsorbed is measured and the data analysis uses the Brunauer-Emmet-Teller isotherm to determine the surface area.

## 4. Modelling

To be able to control the size and shape and thus the properties of the particles produced, it is important to have detailed knowledge of the physical processes involved in particle formation, therefore modelling is needed. In this chapter the modelling tools used in this thesis are briefly described.

Aerosol dynamics is described by an equation termed the general dynamic equation (GDE) [Friedlander 2000]. This equation gives the evolution in time of the size distribution function:

$$\frac{\partial n}{\partial t} + \nabla \cdot (\dot{\vec{x}}n) = -\frac{\partial}{\partial v}(\dot{v}n) + \frac{1}{2} \int_0^v \beta(u, v-u)n(v-u)du - \int_0^\infty \beta(u, v)n(u)n(v)du + J\delta(v-v^*) - k_{DEF}n \quad (1)$$

where  $n$  is the number density function,  $t$  the time,  $\dot{\vec{x}}$  the velocity vector,  $u$  and  $v$  are particle volume,  $\beta$  is the collision frequency function,  $J$  the nucleation rate and  $k_{dep}$  the deposition flux. The terms on the left-hand side of the equation give the temporal and spatial changes in the number density function. The first term on the right-hand side describes condensation, the second and third terms coagulation and the fourth term nucleation. The last term on the right-hand side accounts for losses due to deposition. Since the GDE is a nonlinear, partial integro-differential equation, it is difficult to solve.

In the present work (papers I and II) the aerosol dynamics in silver particle formation and growth via evaporation-condensation was modelled using the GDE. The two different approaches used will be described in subsequent sections.

### 4.1 Sectional method

In paper I the ABC computer code [Jokiniemi et al. 1994] was utilised for numerical solution of the GDE. ABC was initially designed for aerosol size distribution dynamics simulation in combustion processes. Two different

solution models were used: (a) a nucleation-condensation-coagulation model with sectional particle size distribution representation and (b) a monomer-coagulation model with discrete-sectional size distribution. In the monomer-coagulation model it is assumed that all supersaturated silver vapour molecules are stable particles and begin to grow via coagulation.

In the sectional method the particle size distribution is divided into a number of size sections. The particle properties within each size section are assumed to be constant and represented by the sectional midpoint. In the discrete-sectional method the smallest sections are distributed molecule by molecule, corresponding to monomers, dimers, trimers etc., while the larger sections are logarithmically spaced. The biggest drawback with the sectional method is that it suffers from numerical diffusion [Zhang et al. 1999], if the number of sections is not sufficiently large.

Nucleation, the process in which new particles are formed from vapour species, was modelled using the classical nucleation theory with an adjustable prefactor. This theory suggests that a stable cluster is formed when it overcomes the free-energy barrier [Seinfeld and Pandis 1998]. Deposition by vapour condensation, thermophoresis (particle motion induced by a thermal gradient in gas) and Brownian diffusion (random motion due to collisions with gas molecules) were taken into account in the calculations.

## **4.2 Discrete method**

The GDE was solved using a discrete model [Lehtinen and Kulmala 2003] in paper II. In this method the entire particle size distribution is represented by discrete sizes corresponding to monomers, dimers, trimers etc. This method should be free of numerical diffusion problems. However, it is not suitable for modelling large particles, since there is one differential equation for each size, resulting in tremendous computational costs when large size ranges need to be simulated.

In paper II the nucleation was described in accordance with Lushnikov and Kulmala [1998]. They claimed that the formation of a dimer is not possible without the participation of a third molecule (a molecule of carrier gas), the role

of this molecule is simply to remove the excess energy. Without this participation, the requirement for energy and momentum conservation is not fulfilled. In this approach the nucleation rate,  $J$ , can be expressed as a product of the kinetic dimer formation rate and a correction factor that expresses the probability,  $L$ , that a carrier gas molecule is present in the collision of two monomers:

$$J = L \frac{1}{2} \beta_{11} N_1^2. \quad (2)$$

Here  $\beta_{11}$  is the collision frequency function and  $N_1$  the number concentration of monomers. The probability  $L$  was used as a fitting parameter in the calculations in paper II and the deposition was treated as in paper I.

## 5. Experimental results

In this chapter the experimental results of this thesis are summarised. The important aerosol dynamics processes and chemistry occurring in the different systems are discussed. First some general remarks on tubular flow furnaces and especially the one used in this study will be given.

Since the synthesis conditions are easy to control in a tubular flow furnace setup, it provides good control of the particle characteristics and is also ideal for studying the effects of individual parameters on the particle properties. Using this setup, nanoparticles were produced via both the physical and chemical pathways of the gas-to-particle conversion method. The gas is slowly heated in the furnace and the temperature at the outlet is dependent on the flow rate and gas composition.

A rapid decrease in the gas temperature occurs in the thermal insulation zone at the outlet of the furnace. Cooling of the gas after the furnace is dependent on the flow rate and gas composition and can be made even more effective through use of a diluter. Using a porous tube diluter, the losses of particles due to diffusion and thermophoresis can be minimised [Auvinen et al. 2000].

One example of temperature decrease at the centreline when using a porous tube diluter is presented in Figure 2, this was measured from the setup used in this study. In this figure the gas temperature downstream of the furnace is shown as a function of the residence time both for the diluted and the undiluted cases. In this measurement the setpoint of the second block of the furnace was 1400°C, the flow rate was 10 l/min and the dilution ratio was 10. It can be seen that dilution results in a significantly more rapid temperature decrease compared with the undiluted case.

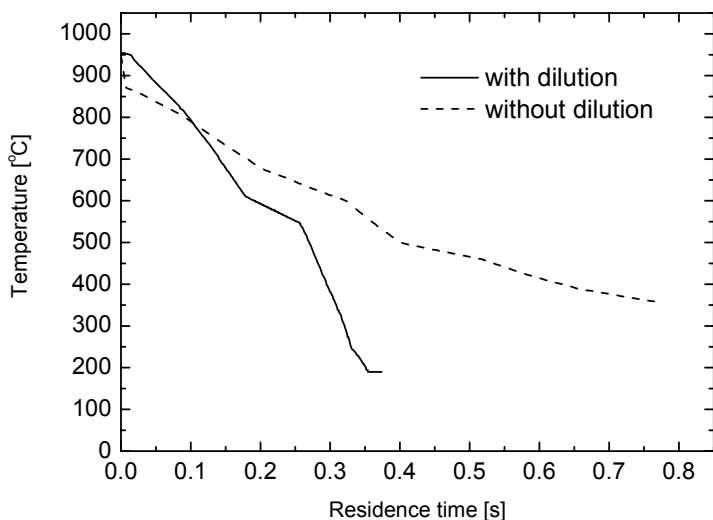


Figure 2. Gas temperature at the centreline downstream of the furnace as a function of the residence time with and without dilution.

## 5.1 Metal nanoparticles

In this study silver nanoparticles were produced via evaporation-condensation. The Ag powder precursor was evaporated in a tubular flow furnace and upon cooling of the vapour downstream, particle formation occurred via nucleation. The effect of quenching on the particle properties was the main focus in paper I.

The silver nanoparticles produced were spherical and nonagglomerated in all the cases studied. A representative TEM image of particles produced using dilution is presented in Figure 3. From the measured number size distribution for the diluted and undiluted cases in Figure 4, it can be seen that by using dilution, smaller and more numerous particles were produced than when no dilution was used. The size varied between 4 and 10 nm, depending on synthesis conditions. The total number concentration was of the order of  $10^8$  particles/cm<sup>3</sup>.

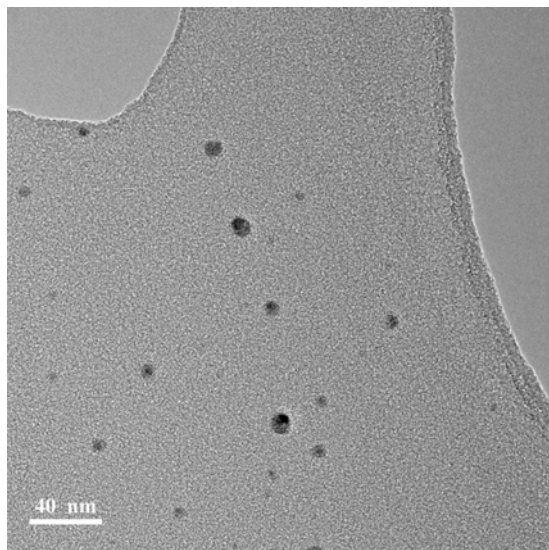


Figure 3. TEM micrograph of silver nanoparticles produced via evaporation-condensation.

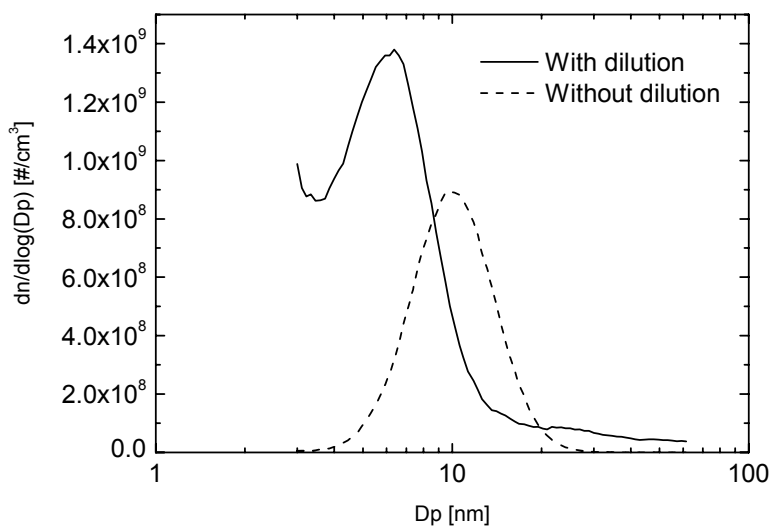


Figure 4. Number size distribution of silver nanoparticles produced with and without dilution.

An example of the influence of quenching on particle formation is presented in Figure 5. When the silver vapour was quenched with dilution gas, very high supersaturation was achieved, which implies high number concentrations of tiny clusters. These tiny clusters first grew mainly by condensation and later, when all vapour was consumed, by agglomeration. If cooling by dilution is sufficient, the agglomerated particles do not sinter and small nanosized primary particles are obtained. Higher temperatures caused the agglomerates to sinter and increase in primary particle size. The temperature required for sintering is strongly dependent on the particle size and material used. In the case of silver the sintering for 10–15 nm particles is rapid even at modest temperatures [Shimada et al. 1994]. Therefore, the particles produced in this study were spherical in all cases.

In the undiluted case (Figure 5) the cooling rate was low and thus fewer and larger stable clusters were formed. The clusters grew by condensation and were thus spherical as long as there was vapour available. After this point, growth by agglomeration is possible if the number concentration is sufficiently high. However, since there is no cooling by dilution, the gas temperature is higher than when dilution is used and if agglomerates are formed, they sinter to form spherical particles. Furthermore, the deposition losses were larger and the particle production rate an order of magnitude lower than when using dilution.

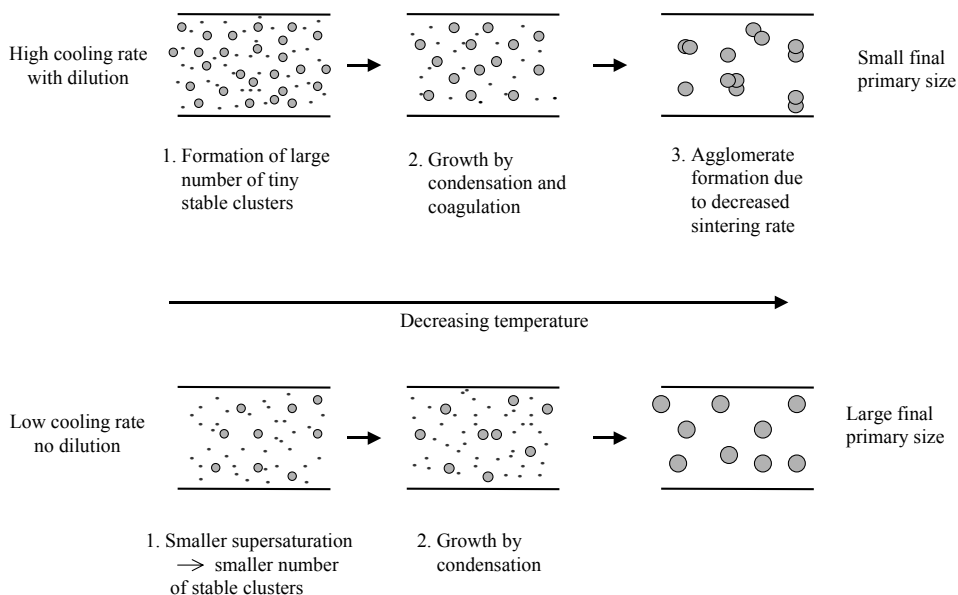
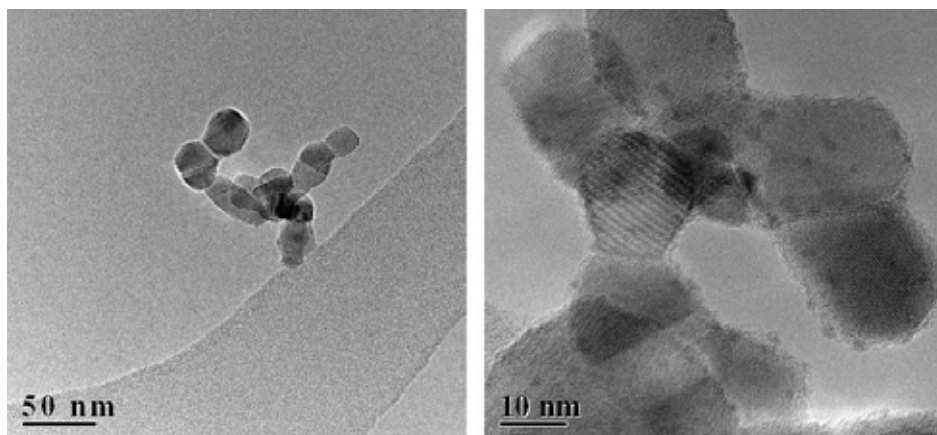


Figure 5. Schematics of silver nanoparticle formation with and without dilution.

## 5.2 Supported metal nanoparticles

In paper III a setup for preparing supported metal catalyst particles in a one-step process was developed. The metal oxide carrier particles were produced via thermal decomposition of a metalorganic precursor and the metal catalyst particles were produced via evaporation-condensation of the metal. The system was tested by preparing Ag/TiO<sub>2</sub> nanoparticles.

The titania particles prepared consisted mainly of those in the anatase phase according to XRD and selected area electron diffraction (SAED) results, with a specific surface area (BET method) between 40 and 92 m<sup>2</sup>/g. The silver mass ratio in the powder prepared at 1100°C was 1.33% as measured with inductively coupled plasma/atomic emission spectrometry (ICP/AES). Typical Ag/TiO<sub>2</sub> nanoparticles are shown in Figure 6. The median size of the silver particles, as



*Figure 6. Agglomerated titania particles (left) and nanometre-sized silver clusters on titania support (right).*

measured from TEM images, was 1.1 nm. In the number size distributions, as measured by DMA/CNC, no peak was detected at particle sizes less than 30 nm, indicating that silver particles were not formed by homogeneous nucleation as was the case without titania, but all the silver was heterogeneously nucleated at the surface of TiO<sub>2</sub> agglomerates.

The schematics of the titania particle dynamics and the silver nucleation discussed in the subsequent paragraphs is presented in Figure 7. When the titania precursor and the N<sub>2</sub> carrier gas was heated in the furnace, the precursor vapour molecules began to decompose forming titania monomers. These monomers quickly formed stable clusters via nucleation due to their low vapour pressure. The titania clusters formed grew by collision with each other and almost immediately coalesced as long as their size was sufficiently small (below about 10 nm, [Kobata et al. 1991]). Several processes occurred simultaneously as the temperature gradually increased, e.g. decomposition of precursor molecules, collision of TiO<sub>2</sub> molecules, clusters and particles formed earlier, as well as CVD (chemical vapour deposition) reactions on the furnace tube and the surface of the particles. When the particles crystallised, their coalescence became slower and was controlled by solid-state diffusion. After this stage the particles were not completely coalesced, i.e. fused together, but instead they formed aggregates of primary particles connected by necks resulting from only partial sintering.

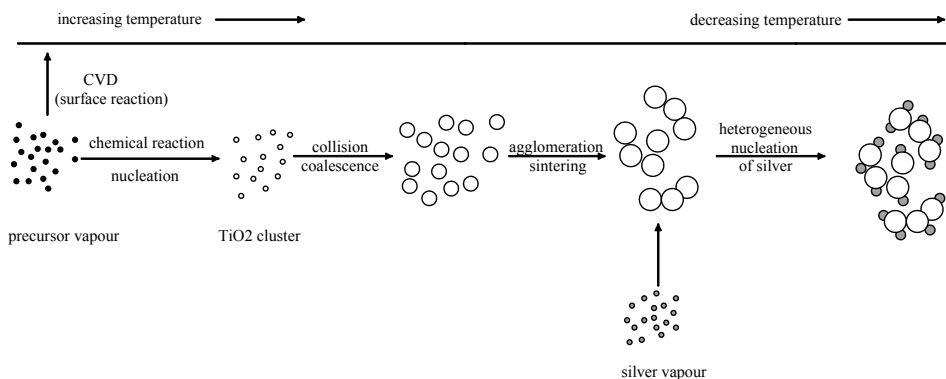


Figure 7. Schematics of titania particle dynamics and silver nucleation.

When the gas was cooled after the furnace, the silver vapour attained its saturation vapour pressure. At this point most of the titania particle dynamics had already occurred and the titania agglomerates were able to serve as nucleation sites, favouring heterogeneous nucleation of silver. The particle size distribution measurements and TEM analyses suggested that the mechanism responsible for Ag particle formation is indeed heterogeneous nucleation on titania agglomerates, because no separate silver particles were observed. The initiation of silver nucleation may have occurred in the cavities of the anatase crystal structure, i.e. not on the surface but few atomic layers deeper in the crystal [Atou et al. 2003].

### 5.3 Deposition of particles with narrow size distribution

In paper IV a simple setup for the deposition of single nonagglomerated particles with a narrow size distribution was developed. The system was tested with titania nanoparticles that were produced via thermal decomposition of a metalorganic precursor. The primary particle size of the spherical particles was about 15 nm. The formation and growth of titania particles was already discussed in chapter 5.2. In the same system films were also deposited via metalorganic chemical vapour deposition (MOCVD), however, these results will not be discussed here.

The setup for deposition of single particles with a narrow size distribution was based on the competition between diffusion and thermophoresis. In the setup used, the gas in the furnace does not reach the temperature of the wall and a temperature gradient exists in the vicinity of the wall. Aerosol particles in a temperature gradient experience a force, thermophoresis, in the direction of decreasing temperature. The thermophoretic velocity is not dependent on the particle size for submicron particles [Hinds 1999], thus all the particles in the system are driven away from the walls of the furnace at the same speed.

Small particles, however, diffuse very rapidly, because the diffusion velocity is strongly dependent on the particle size [Hinds 1999]. Due to this competition between thermophoresis and diffusion, only those particles with a sufficiently high diffusion velocity (the smallest particles) will be able to deposit. This makes the size distribution of the deposited particles narrow and prevents agglomerates from depositing. One example of titania particles deposited in the system is presented in Figure 8. The deposition of this sample occurred at 90 cm from the inlet of the furnace. The particles were deposited on a silicon substrate and analysed as deposited. Size analysis of the deposited particles was performed by measuring the size of 220 particles. The geometric mean diameter of the deposited particles in this case was 13.9 nm, with a geometric standard deviation of 1.33.

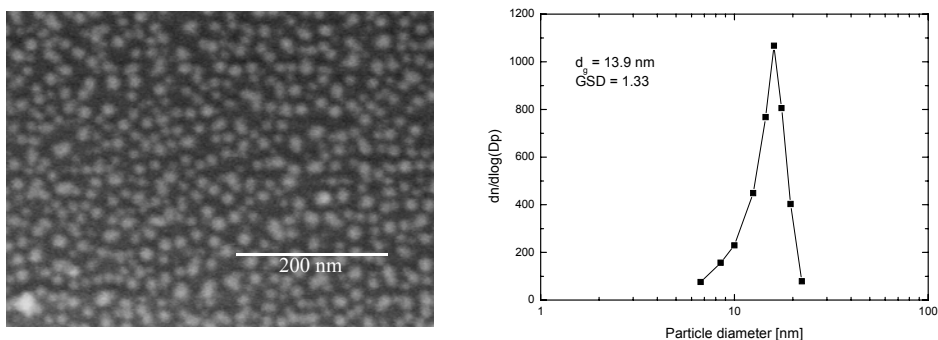


Figure 8. left)  $\text{TiO}_2$  particles with narrow size distribution deposited in setup developed. right) Size distribution of deposited  $\text{TiO}_2$  particles as measured from SEM image.

## 5.4 Synthesis of RuO<sub>2</sub> nanorods

The main objective of paper V was to experimentally study the behaviour of ruthenium at high temperature oxidising conditions. These are the conditions occurring during an air ingress accident in a nuclear power plant. Since the radiotoxicity of ruthenium is high in both the short and long terms it is crucial to understand the transport and speciation of ruthenium under air ingress conditions. However, in this section only the formation of RuO<sub>2</sub> nanorods in the system will be discussed.

RuO<sub>2</sub> powder was used as the precursor in the production of RuO<sub>2</sub> nanorods. Even though the precursor and the final product are the same, this system can be classified as a chemical particle production route since chemical reactions are involved in the processing. Under high temperature oxidising conditions RuO<sub>2</sub> is oxidised to RuO<sub>3</sub> and RuO<sub>4</sub>, both of which are volatile. Since the gaseous ruthenium species are transported to colder regions downstream of the furnace, they become unstable and may decompose to RuO<sub>2</sub> monomers. The RuO<sub>2</sub> monomers formed grow into nanorods.

In the TEM images (Figure 9) it can be seen that the particles were rod-shaped and crystalline. However, since no optimisation of the system or growth conditions was done, the size distribution of the crystals was very broad. Particles were also detected on the walls of the tube. Due to longer residence times, they were larger in size than the particles produced in the gas phase.

This method, the chemical vapour transport technique of growing RuO<sub>2</sub> crystals, was employed by Butler and Gillson [1971], Shafer et al. [1979] and Huang et al. [1982]. They used metallic ruthenium, ruthenium dioxide or a mixture of these as a precursor. The crystals in these experiments were rodlike and millimetre-sized. In some experiments smaller crystals were also observed. The growth times were 10–20 d compared with a maximum of 1 h in our system. The crystal growth mechanism was suggested to be layer spreading [Butler and Gillson 1971].

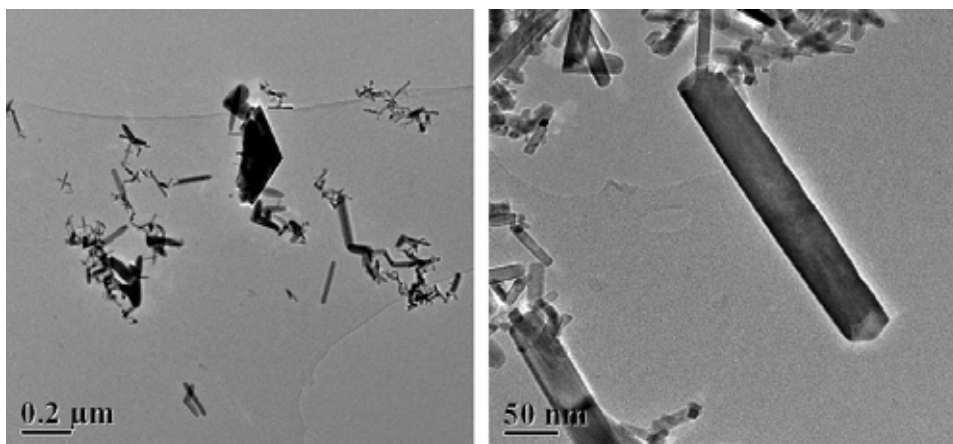


*Figure 9. TEM images of RuO<sub>2</sub> nanorods.*

## 6. Modelling results

In this thesis the formation of silver nanoparticles via gas-to-particle conversion with and without dilution was modelled using two different approaches: in paper I a sectional model and in paper II a discrete model. Nucleation was also described differently: in paper I via the classical nucleation theory with an adjustable prefactor and in paper II with a kinetic model. In this chapter the modelling results are briefly reviewed.

### 6.1 Sectional method

When the diluted case was modelled using the nucleation-condensation-coagulation model and classical nucleation theory, the number size distribution deviated significantly from the measured distribution. However, when the classical nucleation rate was multiplied by a factor of 15 000 the results agreed with the measured values (Figure 10). Classical nucleation theory did not agree with the measured data because the calculated critical radius was only 2.4 Å and bulk properties are not valid for these tiny clusters. The critical radius is the size at which the cluster is in a metastable state; smaller clusters tend to shrink, while larger ones tend to grow. The same calculation was carried out without coagulation and it was observed that coagulation only slightly affects the final particle number size distribution.

The monomer-coagulation model assumes that all supersaturated silver vapour molecules are stable particles and begin to grow by coagulation. This model underestimated the mean size, because after monomer formation growth occurs by particle-particle interaction, which is slower than the condensation that occurs by vapour-particle interaction. This can be explained by the more rapid Brownian movement of vapour molecules compared with particles, due to size effects.

On the other hand, the classical nucleation theory agreed well with the measured size distribution for the undiluted case (Figure 10). In using the nucleation rate as such, nucleation occurs later than if scaling it. Since the temperature gradient and supersaturation are higher at this point more particles are formed than in the

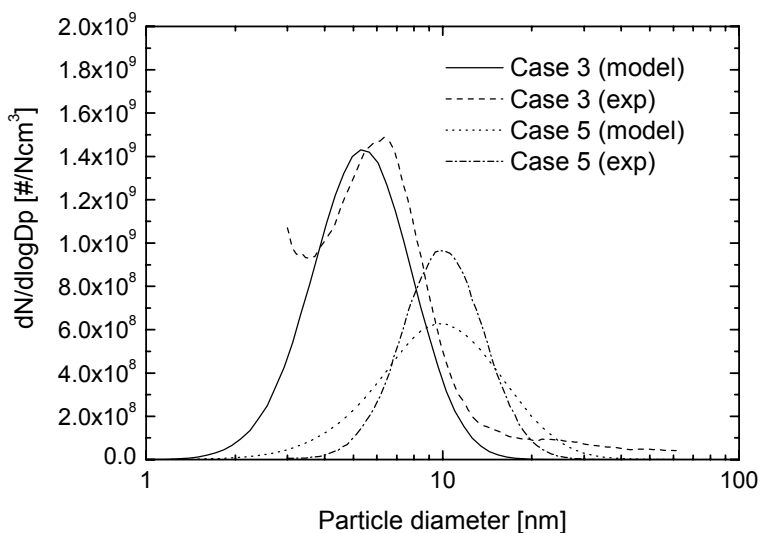


Figure 10. Comparison of experimental and modelling results in the diluted case (case 3) and the undiluted case (case 5). In the diluted case the classical nucleation rate was multiplied by 15 000 whereas in the undiluted case it was used as such.

scaled case and the final size agrees well with the measured value (Figure 10). The monomer-coagulation model now also agreed with the experimental data, but this was probably more an accident than a real physical phenomenon.

Deposition was also modelled and occurred mainly by vapour deposition in both cases. In the diluted case the largest deposition was observed at the flange between the furnace and diluter. In the undiluted case, vapour deposition occurred all the way along the tube. The total deposition for the undiluted case was about 67% of the silver vapour compared with 30% for the diluted case.

It should be noted that there are many simplifying assumptions in the model such as mixing rate, 1-D approximation, surface tension in the condensation model etc. Several sensitivity calculations were carried out by changing the values of parameters that are not precisely known. However, it became clear that the nucleation rate was actually the only critical parameter in modelling the experiments. This result supports the fact that the nucleation rate is crucial for

predicting nanoparticle formation in the evaporation-condensation process and can be interpreted from the experimental results by solving the GDE for various nucleation rates.

## 6.2 Discrete method

In paper II the nucleation of silver nanoparticles was described with a kinetic model. The probability that a carrier gas molecule is present in the collision of two monomers is given by an empirical factor  $L$ . The model was run for different values of this factor to determine if a value exists that can describe the measured size distribution under all experimental conditions. The result for different values of  $L$  in both the diluted (case 3) as well as the undiluted case (case 5) is presented in Figure 11. In the figures the experimentally measured distribution is shown with dots and model results with solid lines.

The best fit, if one wishes to model both cases with the same  $L$ , is accomplished with the choice  $L \sim 8 \cdot 10^{-7}$ , for which the peak location is predicted reasonably well. A distinct visible difference between the experimental and model results is in the width of the distributions obtained: the model produces narrower but higher distributions than those measured. This is because the model is 1-D; i.e. the system undergoes a single set of conditions while traversing through the furnace. However, the collected particle size distribution in reality is a collection from various streamlines, which produces a broader distribution. The difference in the final distributions for the two different cases is also more profound in the experiments than in the model results. The reason for this discrepancy is currently unknown. Still, when compared with the results using classical nucleation theory (paper I), it is clear that this model reproduces the experimental results somewhat better. Using classical nucleation theory, very different corrective factors were needed to model the results: roughly 15 000 for the diluted case and 1 for the undiluted. In addition, the sectional method suffers from numerical diffusion, making the distribution artificially wider. The discrete method avoids this problem.

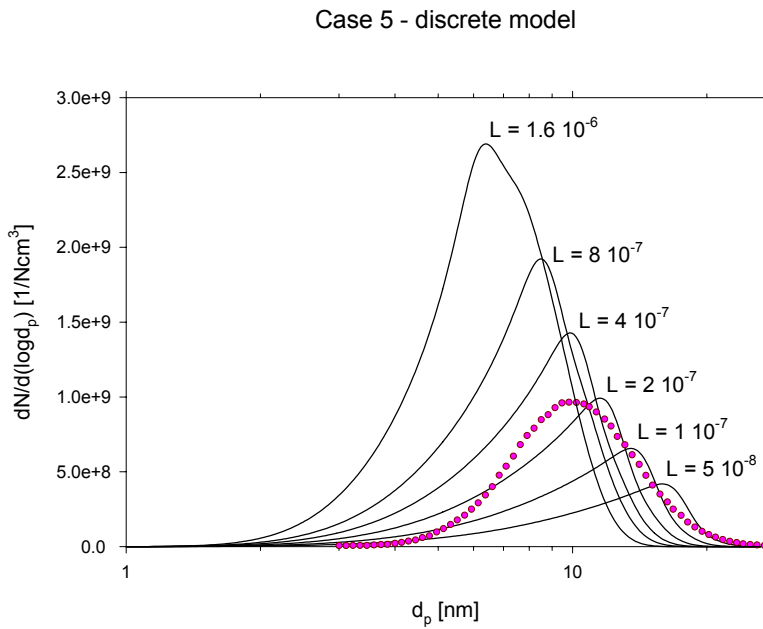
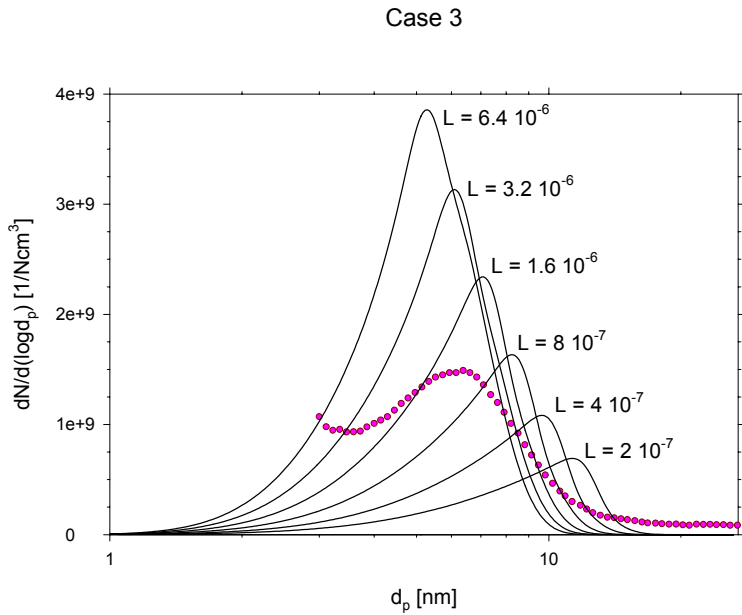


Figure 11. Final number size distributions as a function of particle diameter for the diluted (case 3) and the undiluted case (case 5). The dots represent the experimental results and lines the model results, with different values for the fitting parameter  $L$ .

## 7. Conclusions

In this thesis the synthesis of nanoparticles via aerosol methods was studied both experimentally and theoretically. Particles with controlled properties (i.e. particle size, crystallinity, width of size distribution etc.) were synthesised. In most applications of nanoparticles this is a requirement.

All experiments were carried out using a tubular flow furnace. The nanoparticles were formed via evaporation-condensation or via condensation of reaction products. The evaporation-condensation route is generally cleaner than the chemical route, because no reaction by-products are present in the system. The nanoparticles produced were analysed mainly through use of a DMA/CNC and TEM. The DMA/CNC measured the number size distribution of the particles produced and the morphology, crystallinity and primary particle size of the particles were analysed with the TEM.

Silver nanoparticles were produced via the evaporation-condensation method. The main focus of the study was on how quenching affects the particle properties. In all cases the particles produced were spherical and nonagglomerated, due to the high sintering rate of silver nanoparticles. It was shown that by quenching, more and smaller particles were produced and the losses in the system were smaller.

The development of a single-step aerosol process for producing nanosized supported metal catalytic materials was one aim of this thesis. The system was tested by producing Ag/TiO<sub>2</sub> particles. The silver was well dispersed in 1–2 nm sized particles on the surface of the anatase-phased agglomerated titania particles. The silver concentration in the particles produced was 1.33%. These particles would be excellent as catalysts and photocatalysts since they are anatase-phased. The amount of silver, which increases the photocatalytic activity, would also be suitable. Using aerosol methods, it is possible to control the physico-chemical properties of both the supporting material and the active metal particles by varying the residence time, reactor temperatures and cooling rates.

Using aerosol methods, it is not possible to obtain very narrow particle size distributions, due to Brownian coagulation. However, monodispersed or nearly

monodispersed particles are needed in many applications. One of the aims was to develop a method for deposition of nanoparticles with narrow size distributions. The deposition apparatus relied on the competition between diffusion and thermophoresis. Only particles with diffusion velocities higher than the thermophoretic velocity deposited, i.e. the smallest particles in the size distribution. The size of the single nonagglomerated particles deposited was 13 nm with a geometric standard deviation of 1.33 as measured from the SEM images.

In this thesis RuO<sub>2</sub> nanorods were produced, using the chemical vapour transport technique. At high temperature oxidising conditions ruthenium dioxide reacts to form volatile ruthenium species. As these volatile species cool they decompose, forming RuO<sub>2</sub> nanorods. The size distribution of the nanorods produced was very broad, since no optimisation of the system or growth conditions was carried out.

The aim of the theoretical treatment was to study the formation of silver nanoparticles in detail. The GDE was solved, using different aerosol models. The particle size distribution was represented in two different ways in the modelling: using either sections or discrete molecular resolution. Nucleation was also treated differently in the two cases. In the first case the classical nucleation theory was used and in the second a kinetic model. In the kinetic model it was assumed that a dimer cannot form without the participation of a third molecule (a carrier gas molecule). This molecule is needed to remove the excess energy so that the requirement for energy and momentum conservation is fulfilled.

In this thesis it was shown that for the classical nucleation theory to predict the final particle properties in the various cases very different correction factors, 1–15 000, was needed. The exact reason for the deviation from classical nucleation theory is not known but may be the fact that bulk data are not appropriate for tiny clusters. However, it is a well-known fact that the classical nucleation theory in many cases does not agree with experimental results.

The second nucleation approach used, kinetic nucleation, gave better agreement between the model and the experimental results. This indicates that particle formation may be the result of a dimerisation process. The participation of gas molecules in the initial formation makes the process dependent on total pressure. These results were, likewise, not perfect since the model distributions were too

narrow. In addition, the differences between the diluted and undiluted cases were underestimated.

In the experimental systems and especially in the evaporation-condensation method, the production rate may not always be very high. However, in many applications the quality of the nanoparticles is of the utmost importance and the quantity required may not necessarily be that large, hence the manufacturing costs in these cases do not become insuperable.

There are important issues for further studies to be considered. Catalyst nanoparticles will become increasingly more important and will be used in large quantities. Therefore, scaling-up of the system developed would be needed. The feasibility of producing different combinations of materials is also worth investigating. To be able to deposit particles with even narrower particle size distribution, further development of the system constructed in this thesis would be needed. For ruthenium dioxide nanorods to be used in real applications, the synthesis conditions described should be optimised so that the properties of the crystallites produced are more uniform. In the modelling point of view, a definite answer on the true nucleation mechanism of silver nanoparticles cannot yet be given. One possible improvement may be to couple the used model with a computational fluid dynamics (CFD) simulation routine.

## References

- Agarwal, J. K. and Sem, G. J. 1978. Generating submicron monodisperse aerosols for instrument calibration. *TSI Quarterly*, Vol. 4(2), p. 3–8.
- Atou, Y., Suzuki, H., Kimura, Y., Sato, T., Tanigaki, T., Saito, Y. and Kaito, C. 2003. Novel method for the preparation of silicon oxide layer on TiO<sub>2</sub> particle and dynamic behaviour of silicon oxide layer on TiO<sub>2</sub> particle. *Physica E*, Vol. 16, p. 179–189.
- Auvinen, A., Lehtinen, K. E. J., Enriquez, J. Jokiniemi, J. K. and Zilliacus, R. 2000. Vaporisation rates of CsOH and CsI in conditions simulating a severe nuclear accident. *Journal of Aerosol Science*, Vol. 31(9), p. 1029–1043.
- Baraton, M.-I. and Merhari, L. 2004. Advances in air quality monitoring via nanotechnology. *Journal of Nanoparticle Research*, Vol. 6, p. 107–117.
- Butler, S. R. and Gillson, J. L. 1971. Crystal growth, electrical resistivity and lattice parameters of RuO<sub>2</sub> and IrO<sub>2</sub>. *Materials Research Bulletin*, Vol. 6, p. 81–90.
- Dobosz, A. and Sobczynski, A. 2003. The influence of silver additives on titania photoactivity in the photooxidation of phenol. *Water Research*, Vol. 37, p. 1489–1496.
- Edelstein, A. S. and Cammarata, R. C. (Eds.) 1996. *Nanomaterials: synthesis, properties and applications*. Bristol, Institute of Physics Publishing. 596 p.
- El-Shall, M. S. and Edelstein, A. S. 1996. Formation of clusters and nanoparticles from supersaturated vapor and selected properties. In: Edelstein, A. S. and Cammarat, R. C. *Nanomaterials: synthesis, properties and applications*. Bristol, Institute of Physics Publishing. P. 13–54.
- Friedlander, S. K. 2000. *Smoke, dust and haze: fundamentals of aerosol dynamics*. Second Edition. Oxford University Press, New York.

- Gurav, A., Kodas, T., Pluym, T. and Xiong, Y. 1993. Aerosol processing of materials. *Aerosol Science and Technology*, Vol. 19, p. 411–452.
- Hahn, H. 1997. Gas phase synthesis of nanocrystalline materials. *NanoStructured Materials*, Vol. 9, p. 3–12.
- He, C., Yu, Y., Hu, X. and Larbot, A. 2002. Influence of silver doping on the photocatalytic activity of titania films. *Applied Surface Science*, Vol. 200, p. 239–247.
- Hinds, W. C. 1999. *Aerosol technology: properties, behavior and measurement of airborne particles*, Second edition. New York, John Wiley & Sons. 483 p.
- Huang, Y. S., Park, H. L. and Pollak, F. H. 1982. Growth and characterization of RuO<sub>2</sub> single crystals. *Materials Research Bulletin*, Vol. 17, p. 1305–1312.
- Ichinose, N., Ozaki, Y. and Karsu, S. 1992. *Superfine particle technology*. London, Springer-Verlag. 223 p.
- Jokiniemi, J. K., Lazardis, M., Lehtinen, K. E. J. and Kauppinen, E. I. 1994. Numerical simulation of vapour-aerosol dynamics in combustion processes. *Journal of Aerosol Science*, Vol. 25(3), p. 429–446.
- Kamat, P. V. and Meisel, D. 2003. Nanoscience opportunities in environmental remediation. *C.R. Chimie*, Vol. 6, p. 999–1007.
- Knutson, E. O. and Whitby, K. T. 1975. Aerosol classification by electric mobility: apparatus, theory, and applications. *Journal of Aerosol Science*, Vol. 6, p. 443–451.
- Kobata, A., Kusakabe, K. and Morooka, S. 1991. Growth and transformation of TiO<sub>2</sub> crystallites in aerosol reactor. *AIChE Journal*, Vol. 37(3), p. 347–359.
- Kodas, T. T. and Hampden-Smith, M. J. 1999. *Aerosol processing of materials*. New York. Wiley-VCH. 680 p.

- Kondo, M. M. and Jardim, W. F. 1991. Photodegradation of chloroform and urea using Ag-loaded titanium dioxide as catalyst. *Water Research*, Vol. 25(7), p. 823–827.
- Kruis, F. E., Fissan, H. and Peled, A. 1998. Synthesis of nanoparticles in the gas phase for electronic, optical and magnetic applications – a review. *Journal of Aerosol Science*, Vol. 29(6), p. 511–535.
- Lee, S.-K., Chung, K. W. and Kim, S.-G. 2002. Preparation of various composite TiO<sub>2</sub>/SiO<sub>2</sub> ultrafine particles by vapor-phase hydrolysis. *Aerosol Science and Technology*, Vol. 36, p. 763–770.
- Lehtinen, K. E. J., Windeler, R. S. and Friedlander, S. K. 1996. Prediction of nanoparticle size and the onset of dendrite formation using the method of characteristic times. *Journal of Aerosol Science*, Vol. 27, p. 883–896.
- Lehtinen, K. E. J. and Kulmala, M. 2003. A model for particle formation and growth in the atmosphere with molecular resolution in size. *Atmospheric Chemistry and Physics*, Vol. 3, p. 251–257.
- Lushnikov, A. A. and Kulmala, M. 1998. Dimers in nucleating vapors. *Physical Review E*, Vol. 58(3), p. 3157–3167.
- Penn, S. G., He, L. and Natan M. J. 2003. Nanoparticles for bioanalysis. *Current Opinion in Chemical Biology*, Vol. 7, p. 609–615.
- Pitkethly, M. J. 2003. Nanoparticles as building blocks. *Nanotoday*, December 2003, p. 36–42.
- Seinfeld, J. H. and Pandis, S. N. 1998. *Atmospheric chemistry and physics. From air pollution to climate change.* John Wiley & Sons Inc., New York. 1326 p.
- Shafer, M. W., Figat, R. A., Olson, B., LaPlaca, S. J. and Angilello, J. 1979. Preparation and characterization of ruthenium dioxide crystals. *Journal of the Electrochemical Society*, Vol. 126(9), p. 1625–1628.

Shimada, M., Seto, T. and Okuyama, K. 1994. Size change of very fine silver agglomerates by sintering in a heated flow. *Journal of Chemical Engineering of Japan*, Vol. 27(6), p. 795–802.

Singh, Y., Javier, J. R. N., Ehrman, S. H., Magnusson, M. H. and Deppert, K. 2002. Approaches to increasing yield in evaporation/condensation nanoparticle production. *Journal of Aerosol Science*, Vol. 33, p. 1309–1325.

Swihart, M. T. 2003. Vapor-phase synthesis of nanoparticles. *Current Opinion in Colloid and Interface Science*, Vol. 8, p. 127–133.

Tjong, S. C. and Chen, H. 2004. Nanocrystalline materials and coatings. *Materials Science and Engineering R*, Vol. 45, p. 1–88.

Tsantilis, S. and Pratsinis, S. E. 2004. Soft- and hard-agglomerate aerosols made at high temperatures. *Langmuir*, Vol. 20, p. 5933–5939.

TSI Inc. 1990. Instruction Manual, Model 3025/3027 Ultrafine condensation particle counter. TSI Incorporated.

TSI Inc. 1999. Instruction Manual, Model 3080 electrostatic classifier. TSI Incorporated.

Vamathevan, V., Tse, H., Amal, R. Low, G. and McEvoy, S. 2001. Effects of  $\text{Fe}^{3+}$  and  $\text{Ag}^{+}$  ions on the photocatalytic degradation of sucrose in water. *Catalysis Today*, Vol. 68, p. 201–208.

Wang, S. C. and Flagan, R. C. 1990. Scanning electrical mobility spectrometer. *Aerosol Science and Technology*, Vol. 13, p. 230–240.

Wu, M. K., Windeler, R. S., Steiner, C. K. R., Börs, T. and Friedlander, S. K. 1993. Controlled synthesis of nanosized particles by aerosol processes. *Aerosol Science and Technology*, Vol. 19, p. 527–548.

Yoon, J. D., Park, K. Y. and Jang, H. D. 2003. Comparison of titania particles between oxidation of titanium tetrachloride and thermal decomposition of titanium tetraisopropoxide. *Aerosol Science and Technology*, Vol. 37, p. 621–627.

Zhang, W. 2003. Nanoscale iron particles for environmental remediation: an overview. *Journal of Nanoparticle Research*, Vol. 5, p. 323–332.

Zhang, Y., Seigneur, C., Seinfeld, J. H., Jacobson, M. Z. and Binkowski, F. S. 1999. Simulation of aerosol dynamics: a comparative review of algorithms used in air quality models. *Aerosol Science and Technology*, Vol. 31, p. 487–514.

*Appendices of this publication are not included in the PDF version. Please order the printed version to get the complete publication (<http://www.vtt.fi/inf/pdf>)*

Author(s) Backman, Ulrika			
Title <b>Studies on nanoparticle synthesis via gas-to-particle conversion</b>			
Abstract In the thesis the synthesis of nanoparticles via gas-to-particle conversion was studied both experimentally and theoretically. In the experimental part, nonagglomerated silver nanoparticles were produced via evaporation-condensation. It was shown that it is possible to control the particle size and degree of agglomeration using dilution. A new one-step process for synthesis of supported metal nanoparticles was developed. The metal oxide carrier was produced via thermal decomposition of a metalorganic precursor and the metal was added via evaporation-condensation. The metal was well dispersed in 1–2 nm sized particles on the surface of the agglomerated carrier particles.  A simple system was also developed for depositing single nonagglomerated nanoparticles with a narrow particle size distribution. The system relied on the competition between diffusion and negative thermophoresis. Ruthenium dioxide nanorods were synthesised via decomposition of RuO <sub>3</sub> and RuO <sub>4</sub> vapours.  In the modelling part of this thesis the formation of silver nanoparticles via evaporation-condensation was studied. The modelling was done using two different approaches. The results showed that in order for the classical nucleation theory to predict the final particle properties in the different cases, very different correction factors, 1–15 000, was needed. The kinetic nucleation approach gave better agreement between model and experimental results.			
Keywords nanoparticle synthesis, gas-to-particle conversion, silver nanoparticles, supported metal catalyst nanoparticles, ruthenium dioxide nanorods, aerosol dynamics, characteristics, modelling, deposition, narrow size distribution			
Activity unit VTT Processes, Energy and Environment, Biologinkuja 7, P.O.Box 1602, FI-02044 VTT, Finland			
ISBN 951-38-6441-3 (soft back ed.) 951-38-6442-1 (URL: <a href="http://www.vtt.fi/inf/pdf/">http://www.vtt.fi/inf/pdf/</a> )		Project number	
Date May 2005	Language English	Pages 45 p. + app. 62 p.	Price B
Name of project		Commissioned by	
Series title and ISSN VTT Publications 1235-0621 (soft back ed.) 1455-0849 (URL: <a href="http://www.vtt.fi/inf/pdf/">http://www.vtt.fi/inf/pdf/</a> )		Sold by VTT Information Service P.O.Box 2000, FI-02044 VTT, Finland Phone internat. +358 20 722 4404 Fax +358 20 722 4374	

In this thesis the synthesis of nanoparticles via gas-to-particle conversion was studied both experimentally and theoretically. In the experimental part, metal particles were synthesised via evaporation-condensation and oxide particles via decomposition of a gaseous precursor. A system was also developed for depositing single nonagglomerated nanoparticles with a narrow particle size distribution. The system relied on the competition between diffusion and thermophoresis. In the modelling part, the formation of silver nanoparticles via evaporation-condensation was studied. The results showed that in order for the classical nucleation theory to predict the final particle properties, very different correction factors, 1–15 000, was needed. The kinetic nucleation approach gave better agreement between model and experimental results.

---

Tätä julkaisua myy  
VTT TIETOPALVELU  
PL 2000  
02044 VTT  
Puh. 020 722 4404  
Faksi 020 722 4374

Denna publikation säljs av  
VTT INFORMATIONSTJÄNST  
PB 2000  
02044 VTT  
Tel. 020 722 4404  
Fax 020 722 4374

This publication is available from  
VTT INFORMATION SERVICE  
P.O.Box 2000  
FI-02044 VTT, Finland  
Phone internat. +358 20 722 4404  
Fax +358 20 722 4374